

Mitigating Exposure Bias in Discriminator Guided Diffusion Models

Eleftherios Tsonis, Paraskevi Tzouveli, Athanasios Voulodimos

Artificial Intelligence and Learning Systems Laboratory
School of Electrical and Computer Engineering
National Technical University of Athens

Abstract

Diffusion Models have demonstrated remarkable performance in image generation. However, their demanding computational requirements for training have prompted ongoing efforts to enhance the quality of generated images through modifications in the sampling process. A recent approach, known as Discriminator Guidance, seeks to bridge the gap between the model score and the data score by incorporating an auxiliary term, derived from a discriminator network. We show that despite significantly improving sample quality, this technique has not resolved the persistent issue of Exposure Bias and we propose SEDM-G++, which incorporates a modified sampling approach, combining Discriminator Guidance and Epsilon Scaling. Our proposed approach outperforms the current state-of-the-art, by achieving an FID score of 1.73 on the unconditional CIFAR-10 dataset.

1. Introduction

Diffusion models, initially proposed by Sohl-Dickstein *et al.* in 2015 [41], have excelled in various domains, including image generation, audio generation [7, 25] and video generation [5, 16, 46]. In the domain of image synthesis, diffusion models have seen significant advancements in subsequent years through works such as those of Song and Ermon (2019) [43], Ho *et al.* (2020) [15], and Nichol and Dhariwal (2021) [32]. In 2021, Song *et al.* presented a novel approach that unifies score-based models and Denoising Diffusion Probabilistic Models (DDPMs) by employing stochastic differential equations (SDEs) [44]. Moreover, Karras *et al.* (2022) presented a comprehensive exploration of the diffusion model design space and introduced the EDM model [18], which implemented a range of optimizations to both the sampling and training processes, leading to a substantial enhancement in performance and sample quality.

The computational cost associated with training new

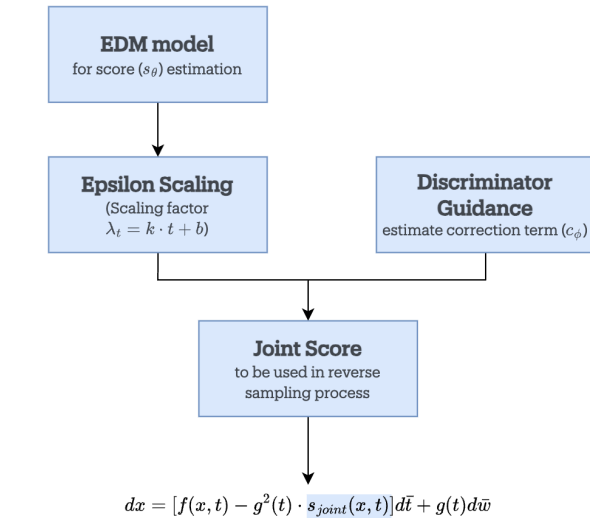


Figure 1. Overview of our proposed SEDM-G++.

score models from the ground up has initiated research endeavors which employ pre-existing score models and enhance the quality of generated samples via refinements in the sampling procedure.

In an effort loosely inspired by Generative Adversarial Networks (GANs), Kim *et al.* [22] modify the diffusion sampling process by utilising a discriminator network to bridge the gap between the model score and the true data score. In their method, *Discriminator Guidance* (DG), they maintain the pre-trained score model as a fixed component and introduce a discriminator network to classify real and generated data across different noise scales. The method incorporates a correction term into the model score, guided by the discriminator’s feedback, which helps steer the sample generation towards more realistic paths.

The iterative sampling chain in diffusion models is long, usually requiring thousands of steps due to the Gaussian assumption of reverse diffusion, which only holds for small

step sizes [41]. This leads to the exposure bias problem, illustrated by Ning *et al.* [35]. Exposure bias refers to the discrepancy between the input data during training and inference phases. During training, the model is consistently exposed to the ground truth training sample \mathbf{x}_t . However, during inference, the model relies on the previously generated sample, $\hat{\mathbf{x}}_t$. This distinction between \mathbf{x}_t and $\hat{\mathbf{x}}_t$ results in a difference between $\epsilon_\theta(\mathbf{x}_t)$ and $\epsilon_\theta(\hat{\mathbf{x}}_t)$, where ϵ_θ is the model’s noise prediction. This disparity between the two predictions results in error accumulation and deviations in the sampling process, known as “sampling drift” [26]. Ning *et al.* [34] propose an effective method, *Epsilon Scaling* for alleviating exposure bias, which is incorporated directly into the sampling process and requires no training or fine-tuning of the model.

The preceding research prompts us to inquire whether Discriminator Guidance is effective in mitigating the accumulation of exposure bias in the sampling process. Our findings indicate that, despite notable enhancements in sample quality, Discriminator Guidance is ineffective in alleviating exposure bias in Diffusion Models. We propose SEDM-G++, which incorporates a modified sampling approach, combining Discriminator Guidance and Epsilon Scaling. Fig. 1 shows an overview of SEDM-G++. We test our method on top of the pre-trained EDM model [18] and show that the proposed sampling process achieves improved sample quality, while reducing exposure bias.

Our contributions can be summarized as follows.

- We investigate exposure bias in discriminator guided diffusion models.
- We propose SEDM-G++, which incorporates a sampling approach combining Discriminator Guidance and Epsilon Scaling.
- Our proposed method improves sample quality across the board and outperforms the current state-of-the-art, by achieving an FID score of 1.73 on the unconditional CIFAR-10 dataset.

We intend to make the code publicly available, upon publication.

2. Related Work

Diffusion models [41] have demonstrated exceptional performance across diverse domains such as image, audio, and video generation [5, 7, 16, 25, 46]. In the realm of image synthesis, substantial progress has been made in recent years through various contributions [6, 15, 17, 18, 30, 32, 38, 42–44]. Diffusion models find a wide range of applications, including text to image generation [14, 27, 39], image inpainting [10, 28, 38, 47], image editing [2, 9, 10, 19, 23, 31, 36], super-resolution [10, 13], point cloud generation [29], 3D shape generation [49] and vision decoding [8].

Ning *et al.* [35] identify a phenomenon associated with

the sampling chain, which involves the accumulation of errors across T inference sampling steps. This accumulation is primarily attributed to the discrepancy between the training and inference stages. During training, the diffusion model is trained with a ground truth pair $(\mathbf{x}_t, \mathbf{x}_{t-1})$, learning to reconstruct \mathbf{x}_{t-1} given \mathbf{x}_t . However, during inference, the model lacks access to the ground truth \mathbf{x}_t and relies on the previously generated $\hat{\mathbf{x}}_t$, leading to a potential accumulation of errors. This mismatch between the input used in training and the input used in sampling resembles the exposure bias problem, originally observed in other generative models [37, 40].

To address the exposure bias issue, Ning *et al.* [35] suggest explicitly modeling the prediction error during training. During the training phase, they perturb \mathbf{x}_t as normal and provide the network with a new, noisier version of \mathbf{x}_t . This simulates the training-sampling discrepancy, fooling the learned network into considering potential prediction errors during inference. Even though their method proves effective in reducing the exposure bias phenomenon, it is cumbersome as it necessitates retraining the score network entirely, a computationally expensive endeavor.

Li *et al.* [26] propose a different approach, which involves shifting the timestep t during sampling. They observe that the time step t is directly linked to the corruption level of data samples, and demonstrate that adjusting the subsequent time step $t - 1$ during sampling, based on the variance of the currently generated samples, can effectively mitigate exposure bias. Despite the fact that their method circumvents the need for model retraining, tuning the timestep shift is difficult to optimize.

3. Background

3.1. Diffusion Models Framework

In DDPMs, Ho *et al.* [15] define the forward diffusion process as the gradual addition of noise to a clean datum, until structure is destroyed entirely and the datum is transformed into pure noise. Consider the data distribution $\mathbf{x}_0 \sim q(\mathbf{x}_0)$. The forward process is essentially a Markov chain, which generates a sequence of random variables $\mathbf{x}_1, \mathbf{x}_2, \dots, \mathbf{x}_T$ with transition kernel $q(\mathbf{x}_t|\mathbf{x}_{t-1})$. A variance schedule $\{\beta_t \in (0, 1)\}_{t=0}^T$, such that the noise perturbing the data at each discrete timestep t is an isotropic Gaussian with variance β_t , is inherent to the DDPM framework. The Markov chain is defined by the transition kernel:

$$q(\mathbf{x}_t|\mathbf{x}_{t-1}) = \mathcal{N}(\mathbf{x}_t; \sqrt{1 - \beta_t}\mathbf{x}_{t-1}, \beta_t\mathbf{I}) \quad (1)$$

The joint distribution of $\mathbf{x}_1, \mathbf{x}_2, \dots, \mathbf{x}_T$, conditioned on \mathbf{x}_0 is:

$$q(\mathbf{x}_{1:T}|\mathbf{x}_0) = \prod_{t=1}^T q(\mathbf{x}_t|\mathbf{x}_{t-1}) \quad (2)$$

A significant quality of the forward diffusion process is that \mathbf{x}_t , drawn from $q(\mathbf{x}_t|\mathbf{x}_{t-1})$ at timestep t , can be directly expressed as a linear combination of \mathbf{x}_0 and a noise variable $\epsilon \sim \mathcal{N}(\mathbf{0}, \mathbf{I})$:

$$\mathbf{x}_t = \sqrt{\bar{a}_t}\mathbf{x}_0 + \sqrt{1 - \bar{a}_t}\epsilon \quad (3)$$

where $\bar{a}_t = \prod_{i=1}^t(1 - \beta_i)$ and $\alpha_t = 1 - \beta_t$.

For the reverse process, seeing as estimating $q(\mathbf{x}_{t-1}|\mathbf{x}_t)$ is unfeasible, a learnable transition kernel p_θ is utilised instead, to approximate the conditional probabilities. The kernel takes the following form:

$$p_\theta(\mathbf{x}_{t-1}|\mathbf{x}_t) = \mathcal{N}(\mathbf{x}_{t-1}; \mu_\theta(\mathbf{x}_t, t), \Sigma_\theta(\mathbf{x}_t, t)) \quad (4)$$

where θ denotes model parameters. By sampling $\mathbf{x}_T \sim \mathcal{N}(\mathbf{0}, \mathbf{I})$ and iteratively using Eq. 4 to run the reverse diffusion process, we obtain a sample from $q(\mathbf{x}_0)$.

The success of the sampling process depends on training the reverse Markov chain to match the time reversal of the forward Markov chain. This involves adjusting parameter θ to make the joint distribution of the reverse Markov chain $p_\theta(\mathbf{x}_{0:T}) = p(\mathbf{x}_T) \prod_{t=1}^T p_\theta(\mathbf{x}_{t-1}|\mathbf{x}_t)$ closely approximate the joint distribution of the forward process $q(\mathbf{x}_{0:T}) = q(\mathbf{x}_0) \prod_{t=1}^T q(\mathbf{x}_t|\mathbf{x}_{t-1})$ (Eq. 2). This is accomplished by minimizing the Kullback-Leibler (KL) divergence between $p_\theta(\mathbf{x}_{t-1}|\mathbf{x}_t)$ and $q(\mathbf{x}_{t-1}|\mathbf{x}_t, \mathbf{x}_0)$:

$$D_{KL}(q(\mathbf{x}_{t-1}|\mathbf{x}_t, \mathbf{x}_0) || p_\theta(\mathbf{x}_{t-1}|\mathbf{x}_t)) \quad (5)$$

Ho *et al.* show that it is possible to directly compare $p_\theta(\mathbf{x}_{t-1}|\mathbf{x}_t)$ against forward process posteriors, which are tractable when conditioned on \mathbf{x}_0 [15]:

$$q(\mathbf{x}_{t-1}|\mathbf{x}_t, \mathbf{x}_0) = \mathcal{N}(\mathbf{x}_{t-1}; \tilde{\mu}_t(\mathbf{x}_t, \mathbf{x}_0), \tilde{\beta}_t \mathbf{I}), \quad (6)$$

where:

$$\tilde{\mu}_t(\mathbf{x}_t, \mathbf{x}_0) = \frac{\sqrt{\bar{\alpha}_{t-1}}\beta_t}{1 - \bar{\alpha}_t}\mathbf{x}_0 + \frac{\sqrt{\alpha_t}(1 - \bar{\alpha}_{t-1})}{1 - \bar{\alpha}_t}\mathbf{x}_t \quad (7)$$

$$\tilde{\beta}_t = \frac{1 - \bar{\alpha}_{t-1}}{1 - \bar{\alpha}_t}\beta_t \quad (8)$$

By plugging Eq. 3 into Eq. 7 we derive that given \mathbf{x}_t , μ_θ must predict the following quantity:

$$\mu_\theta(\mathbf{x}_t, t) = \frac{1}{\sqrt{a_t}} \left(\mathbf{x}_t - \frac{\beta_t}{\sqrt{1 - \bar{a}_t}} \epsilon_\theta(\mathbf{x}_t, t) \right) \quad (9)$$

where ϵ_θ is the approximate prediction for noise factor ϵ based on \mathbf{x}_t .

3.2. Stochastic Differential Equations

Song *et al.* [44] demonstrated that DDPMs can be regarded as discretizations of stochastic differential equations (SDEs), thus providing a unifying perspective on previous

approaches. The forward diffusion process is described by the forward SDE:

$$d\mathbf{x} = \mathbf{f}(\mathbf{x}, t)dt + g(t)d\mathbf{w}, \quad (10)$$

where $\mathbf{f}(\mathbf{x}, t)$ is the drift coefficient, $g(t)$ is the diffusion coefficient and t is a continuous time variable in $[0, T]$.

Anderson [1] demonstrated that reversing a diffusion process yields another diffusion process, which operates backward in time and is described by the reverse-time stochastic differential equation:

$$d\mathbf{x} = [\mathbf{f}(\mathbf{x}, t) - g^2(t)\nabla \log q(\mathbf{x})]d\bar{t} + g(t)d\bar{\mathbf{w}}, \quad (11)$$

where $d\bar{t}$ and $d\bar{\mathbf{w}}$ denote the infinitesimal reverse-time and reverse-time Brownian motion, respectively. Consequently, the continuous-time generative process is formulated as:

$$d\mathbf{x} = [\mathbf{f}(\mathbf{x}, t) - g^2(t)\mathbf{s}_\theta(\mathbf{x}, t)]d\bar{t} + g(t)d\bar{\mathbf{w}}, \quad (12)$$

Here, the score network's estimation target $\mathbf{s}_\theta(\mathbf{x}, t)$ corresponds to the actual data score $\nabla \log q(\mathbf{x})$.

3.3. Discriminator Guidance

We investigate Exposure Bias in the discriminator guided EDM-G++ (Kim *et al.* [22]). Their approach keeps the score function frozen and trains a discriminator network in isolation. The absence of adversarial training makes convergence simpler and faster to achieve, compared to GANs. When producing samples using the reverse-time SDE:

$$d\mathbf{x} = [\mathbf{f}(\mathbf{x}, t) - g(t)^2\mathbf{s}_{\theta_\infty}(\mathbf{x}, t)]dt + g(t)d\bar{\mathbf{w}} \quad (13)$$

Kim *et al.* [22] show that the generative process might diverge from the reverse-time data process if the local optimum θ_∞ of the score network $\mathbf{s}_{\theta_\infty}$ is different to the global optimum θ_* . However, augmenting the score function by a *correction term* can bridge the gap between the two processes.

The reverse-time SDE with the adjusted score becomes:

$$d\mathbf{x} = [\mathbf{f}(\mathbf{x}, t) - g(t)^2(\mathbf{s}_{\theta_\infty} + \mathbf{c}_{\theta_\infty})(\mathbf{x}, t)]dt + g(t)d\bar{\mathbf{w}} \quad (14)$$

for $\mathbf{c}_{\theta_\infty}(\mathbf{x}, t) = \nabla \log \frac{p_r^t(\mathbf{x})}{p_{\theta_\infty}^t(\mathbf{x})}$. Seeing as this correction term is intractable, Kim *et al.* [22] train a neural discriminator d_{ϕ_*} at all noise levels t and use it to estimate the correction term $\mathbf{c}_{\theta_\infty}$:

$$\mathbf{c}_{\theta_\infty}(\mathbf{x}, t) \approx \mathbf{c}_{\phi_\infty}(\mathbf{x}, t) = \nabla \log \frac{d_\phi(\mathbf{x}, t)}{1 - d_\phi(\mathbf{x}, t)} \quad (15)$$

Thus, they define the discriminator guided reverse SDE as:

$$d\mathbf{x} = [\mathbf{f}(\mathbf{x}, t) - g(t)^2(\mathbf{s}_{\theta_\infty} + \mathbf{c}_\phi)(\mathbf{x}, t)]dt + g(t)d\bar{\mathbf{w}}. \quad (16)$$

The Exposure Bias problem has been uncovered in traditional DDPMs, DDIMs and other diffusion models [26, 34, 35] but not yet in the Discriminator Guidance approach.

3.4. Prediction Error leads to Exposure Bias

The exposure bias problem in diffusion models, highlighted by Ning *et al.* [35], refers to the mismatch between the model’s input data during the training and the inference phase. During training, the ground truth training sample \mathbf{x}_t is available to the model, with the training distribution being $q(\mathbf{x}_t|\mathbf{x}_0)$. In the inference phase, the model can only rely on the previously generated sample, $\hat{\mathbf{x}}_t$. The sampling distribution can be denoted as $q(\hat{\mathbf{x}}_t|\mathbf{x}_{t+1}, \mathbf{x}_\theta^{t+1})$, where \mathbf{x}_θ^{t+1} is the prediction the model makes for \mathbf{x}_0 given \mathbf{x}_{t+1} , using Eq. 3, following notation by Ning *et al.* [34]. This results in a discrepancy between $\epsilon_\theta(\mathbf{x}_t)$ and $\epsilon_\theta(\hat{\mathbf{x}}_t)$.

Xiao *et al.* [48] observed that the sampling distribution $p_\theta(\mathbf{x}_{t-1}|\mathbf{x}_t)$ is parameterized as:

$$p_\theta(\mathbf{x}_{t-1}|\mathbf{x}_t) = q(\mathbf{x}_{t-1}|\mathbf{x}_t, \mathbf{x}_\theta^t) \quad (17)$$

where \mathbf{x}_θ^t represents the predicted \mathbf{x}_0 . The sampling process involves predicting ϵ using $\epsilon_\theta(\mathbf{x}_t, t)$ and deriving the estimation \mathbf{x}_θ^t for \mathbf{x}_0 using Eq. 3. Then, \mathbf{x}_{t-1} is generated based on the ground truth posterior $q(\mathbf{x}_{t-1}|\mathbf{x}_t, \mathbf{x}_0)$, by replacing \mathbf{x}_0 with \mathbf{x}_θ^t . However, $q(\mathbf{x}_{t-1}|\mathbf{x}_t, \mathbf{x}_0) = q(\mathbf{x}_{t-1}|\mathbf{x}_t, \mathbf{x}_\theta^t)$ holds only if $\mathbf{x}_\theta^t = \mathbf{x}_0$. In practice, $q(\mathbf{x}_{t-1}|\mathbf{x}_t, \mathbf{x}_0) \neq q(\mathbf{x}_{t-1}|\mathbf{x}_t, \mathbf{x}_\theta^t)$, as the network makes prediction errors when estimating \mathbf{x}_0 and, as a result, $q(\mathbf{x}_{t-1}|\mathbf{x}_t, \mathbf{x}_\theta^t)$ does not have the same variance as $q(\mathbf{x}_{t-1}|\mathbf{x}_t, \mathbf{x}_0)$.

Ning *et al.* [34] analytically calculate the discrepancy between the training and sampling distribution in DDPMs. They model \mathbf{x}_θ^t as $p_\theta(\mathbf{x}_0|\mathbf{x}_t)$ and approximate it by a Gaussian distribution, following Bao *et al.* [3, 4].

$$\mathbf{x}_\theta^t = \mathbf{x}_0 + e_t \epsilon_0 \quad (18)$$

where e_t is the standard deviation of \mathbf{x}_θ^t and $\epsilon_0 \sim \mathcal{N}(\mathbf{0}, \mathbf{I})$. Their findings are summarized in Table 1. It becomes clear that the sampling distribution’s variance is always larger than that of the training distribution by a factor of $(\frac{\sqrt{\bar{\alpha}_t \beta_{t+1}}}{1 - \bar{\alpha}_{t+1}} e_{t+1})^2$. It must be noted that this is the prediction error produced in a single reverse diffusion step. During sampling, the errors accumulate across steps, resulting in the Exposure Bias problem.

	Mean	Variance
$q(\mathbf{x}_t \mathbf{x}_0)$	$\sqrt{\bar{\alpha}_t} \mathbf{x}_0$	$(1 - \bar{\alpha}_t) \mathbf{I}$
$q(\hat{\mathbf{x}}_t \mathbf{x}_{t+1}, \mathbf{x}_\theta^{t+1})$	$\sqrt{\bar{\alpha}_t} \mathbf{x}_0$	$(1 - \bar{\alpha}_t + (\frac{\sqrt{\bar{\alpha}_t \beta_{t+1}}}{1 - \bar{\alpha}_{t+1}} e_{t+1})^2) \mathbf{I}$

Table 1. Mean and variance of $q(\mathbf{x}_t|\mathbf{x}_0)$ and $q(\hat{\mathbf{x}}_t|\mathbf{x}_{t+1}, \mathbf{x}_\theta^{t+1})$

3.5. Epsilon Scaling

Ning *et al.* [34] propose scaling down the predicted noise factor ϵ_θ^s (where s denotes the noise factor predicted in the

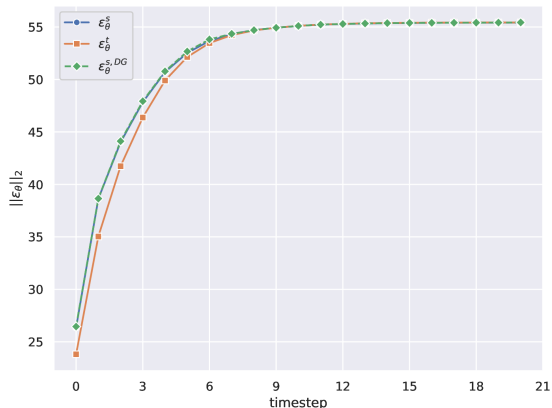


Figure 2. EDM model, Euler 1st order solver. L_2 -norm of $\epsilon_\theta(\cdot)$ during 21-step sampling, sampling with DG and training. Statistical L_2 -norm was calculated using 50k samples at each timestep. Sampling is from right to left.

sampling stage) by a factor λ_t at time step t as a way to reduce Exposure Bias. Their approach is based on the assumption that the accuracy of the prediction ϵ_θ^s can be enhanced if we are able to shift the input ($\hat{\mathbf{x}}_t, t$) away from the unreliable vector field (depicted as the orange curve in Fig. 2 and 3) and towards the dependable vector field (represented by the green curve in Fig. 2 and 3).

Their approach is rooted in the following observation: ϵ_θ^s and ϵ_θ^t (where t denotes to the noise factor predicted in the training stage) both originate from the same input $\mathbf{x}_T \sim \mathcal{N}(0, \mathbf{I})$ at time step $t = T$. However, starting from time step $T - 1$, $\hat{\mathbf{x}}_t$ (the input for ϵ_θ^s) begins to deviate from \mathbf{x}_t (the input for ϵ_θ^t) due to the $\epsilon_\theta(\cdot)$ error made in the previous time step. This iterative process continues throughout the sampling chain, leading to exposure bias. Therefore, we can bring $\hat{\mathbf{x}}_t$ closer to \mathbf{x}_t by reducing the overestimated magnitude of ϵ_θ^s . Their sampling method only differs from Eq. 9 in the λ_t term and can be expressed as:

$$\mu_\theta(\mathbf{x}_t, t) = \frac{1}{\sqrt{a_t}} \left(\mathbf{x}_t - \frac{\beta_t}{\sqrt{1 - \bar{a}_t}} \frac{\epsilon_\theta(\mathbf{x}_t, t)}{\lambda_t} \right) \quad (19)$$

As a result, epsilon scaling is a plug-in method which requires no retraining or fine-tuning of the original score model and adds no overhead computational cost.

4. Method

4.1. Quantifying Exposure Bias

As Table 1 illustrates, the \mathbf{x}_t seen by the network during training differs from the $\hat{\mathbf{x}}_t$ seen by the network during sampling. This discrepancy leads to a drift between the noise prediction made during training, ϵ_θ^t , and the noise predic-

tion made during sampling, ϵ_{θ}^s . Following Ning *et al.* [34], we choose to measure the sampling drift at each timestep as the difference between ϵ_{θ}^t and ϵ_{θ}^s . However, since the ground truth of ϵ_{θ}^s is intractable in the sampling phase, we use the L_2 -norm to quantify the exposure bias [34].

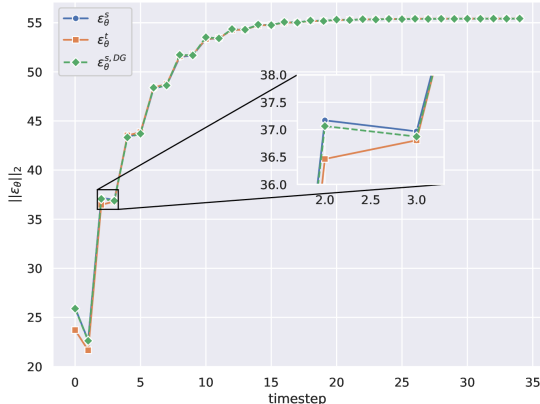


Figure 3. EDM model, Heun 2nd order solver. L_2 -norm of $\epsilon_{\theta}(\cdot)$ during 35-step sampling, sampling with DG and training. Statistical L_2 -norm was calculated using 50k samples at each timestep. Sampling is from right to left.

In Fig. 2 and Fig. 3 we plot the L_2 -norm of ϵ_{θ}^t , ϵ_{θ}^s and $\epsilon_{\theta}^{s,DG}$ using the Euler, as well as the Heun ODE solver. ϵ_{θ}^s and $\epsilon_{\theta}^{s,DG}$ refer to the noise prediction in the vanilla EDM model and in the discriminator guided EDM-G++ model, respectively. We observe that in the case of the Euler solver, the L_2 -norm of $\epsilon_{\theta}^{s,DG}$ is larger than that of ϵ_{θ}^t and nearly coincides with the L_2 -norm of ϵ_{θ}^s . In the case of the Heun 2nd order solver, the difference between the two norms is smaller, however, the L_2 -norm of $\epsilon_{\theta}^{s,DG}$ is, once again, larger than that of ϵ_{θ}^t and closer to that of ϵ_{θ}^s . This means that the correction term offered by discriminator guidance does not alleviate the sampling procedure of its collected exposure bias. Instead, the prediction errors accumulate and the learnt vector field $\epsilon_{\theta}^{s,DG}$ deviates from the desired sampling trajectory.

4.2. Proposed Framework

We use the EDM model, proposed by Karras *et al.* [18], as a score estimator due to the detailed way in which it was designed. Through careful network design and fine-tuning of hyperparameters, EDM achieves a substantial quality enhancement, reducing the FID score on the CIFAR-10 dataset to 1.97, demonstrating notable progress at the time. Moreover, seeing as Exposure Bias exhibits a strong correlation with FID score [34], we assume that in comparison to other networks, the vanilla EDM model demonstrates a reduced accumulation of exposure bias.

When it comes to the discriminator network, we follow the setup demonstrated by Kim *et al.* [22]. The discriminator network is comprised of the encoders of two U-Net structures. The first U-Net encoder is frozen and the second one is fine-tuned, to accelerate training. We leave the exploration of other discriminator architectures, such as Vision Transformers, as future work.

In Sec. 2, we mention different approaches which seek to reduce the impact of Exposure Bias on the sampling trajectory. Ning *et al.* [35] suggest introducing an extra noise factor at each step during the training to mitigate the discrepancy between training and inference. However, this method proves cumbersome as it requires retraining the model from scratch. Li *et al.* [26] explore how manipulation of the time step during the reverse generation process can trick the model into reducing the Exposure Bias issue. This method is also difficult to implement as exploring the entire space of possible combinations is inconvenient as it requires costly experimentation to produce noteworthy results. The latest method to reduce Exposure Bias, introduced by Ning *et al.* [34], known as Epsilon Scaling, is our selected approach. It is a training free, plug-in method, which has proven effective in reducing Exposure Bias and significantly improving the FID score across a range of diffusion models (ADM [11], DDIM [42], EDM [18], LDM [38]). We present the main notion of Epsilon Scaling in Sec. 3.5.

Although the network output of EDM is the score function s_{θ} , not ϵ , the noise factor ϵ can easily be extracted at each sampling step and used to apply Epsilon Scaling [34].

When it comes to designing the scaling schedule λ_t , Ning *et al.* [34] propose that the term λ_t should be a linear function $\lambda_t = kt + b$ where k, b are constants. They also observe that the longer the sampling step, the smaller the k that should be used. Thus, they suggest a uniform schedule $\lambda_t(k = 0)$ to facilitate practicality and simplify the exploration of the b parameter. In our experiments, we confirm that the use of a linear λ_t can provide similar or sub-optimal results, compared to the uniform schedule $\lambda_t = b$ and explore the constant scaling factor more extensively.

5. Results

5.1. Euler Solver

We firstly present our results using the Euler 1st order ODE solver. When it comes to the Discriminator Guidance method (Kim *et al.* [22]), we identify a noteworthy omission. Namely, the authors do not report performance of the EDM-G++ model using the Euler ODE solver. We have calculated the FID score of EDM-G++ on the CIFAR-10 dataset using various numbers of timesteps and Discriminator Guidance weight, w^{DG} and we present our results in Fig. 4.

Notably, the EDM-G++ model, which is guided by a dis-

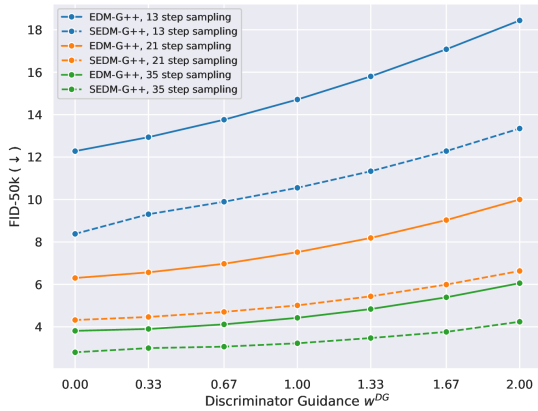


Figure 4. FID-50k ablation study on DG weight (Euler Solver).

criminator, exhibits a noteworthy decrease in sample quality when compared to the baseline EDM model. This decline intensifies as the weight assigned to the discriminator’s correction term, w^{DG} , increases. This outcome is intriguing in light of the fact that the inclusion of discriminator guidance led to a substantial reduction in the FID score using the Heun 2nd order ODE solver. It is plausible to surmise that the reduced FID score in the case of the 1st order solver may be attributed to the absence of a corrective step in the sampling process. The enhancement of sample quality in the EDM model [18] is markedly facilitated by the inclusion of a corrective step in the ODE solver. This is a crucial factor contributing to the widespread adoption of the Heun ODE solver in recent research, as it consistently delivers superior performance [18].

Nevertheless, the epsilon scaling method demonstrates its efficacy in the context of discriminator-guided diffusion models as well. SEDM-G++ successfully reduces the FID score across different numbers of total timesteps and w^{DG} values when utilizing the Euler ODE solver, as compared to the EDM-G++ and EDM baselines. Remarkably, SEDM-G++ narrows the performance gap between EDM-G++ using a 21-step Euler solver and a 35-step Euler solver, with the performance of SEDM-G++ using a 21-step Euler solver closely approaching that of the baseline EDM-G++ model using a 35-step Euler solver. This results in a significant reduction in computational and time requirements during inference, without compromising sample quality to a considerable extent.

In Figure 5, we present uncoordinated samples derived from the EDM-G++ baseline and our proposed SEDM-G++. Apart from the evident improvement in the FID score, our method yields noticeable qualitative enhancements in the generated samples. For example, the sample located in the third row and third column, as well as the sample in the

fifth row and fourth column, exhibit a substantial enhancement compared to the baseline. In Figure 5a, the shapes appear blurry and obscure, making it challenging to discern the content of the images. Conversely, in Figure 5b, SEDM-G++ produces images with clear, well-defined shapes and vivid colors, rendering the identity of the depicted objects readily discernible.

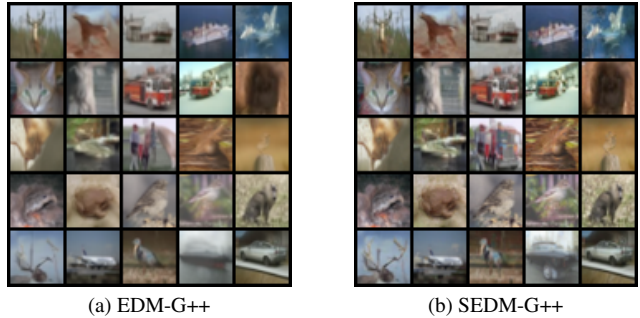


Figure 5. Uncoordinated samples from the EDM-G++ baseline and our proposed SEDM-G++.

5.2. Heun Solver

We further explore the performance of SEDM-G++ using the Heun 2nd order ODE solver. We conducted an ablation study on the relation between the weight attributed to discriminator guidance in the 1st order step of the Heun solver, namely $w_{t,1st}^{DG}$, and the epsilon scaling factor $\lambda_t = b$. Based on the work of Kim *et al.* [22], we set the 2nd order discriminator guidance weight, namely $w_{t,2nd}^{DG}$ equal to zero for all tests. This choice offers optimal sample quality and requires fewer computational resources, as the number of calls to the discriminator network is practically halved by omission in the 2nd order corrective steps. In order to reduce the computational needs of our study, rather than generating a total of 50k samples, we generate 10k samples for each setting and derive the FID-10k score, which suffices for the purpose of parameter optimization [34]. The results are presented in Fig. 6.

Our observations indicate that the most effective discriminator guidance weight values are 1.67 and 2. Notably, when comparing these two values, we also note that the optimal epsilon scaling value λ_t decreases as the discriminator’s weight coefficient increases. We further delve into the performance of the best-performing $w_{t,1st}^{DG}$ values through a comprehensive study, by generating 50k samples for each setting and utilizing the proper FID-50k score to compare. We present our results in Fig. 7.

Our proposed SEDM-G++ outperforms the current state-of-the-art in unconditional CIFAR-10 image generation, by achieving an FID score of 1.73. The optimal hyperparameters used are $\lambda_t = 1.0004$, $w_{t,1st}^{DG} = 1.67$ and $w_{t,2nd}^{DG} = 0$. A comprehensive comparison between SEDM-G++ and other

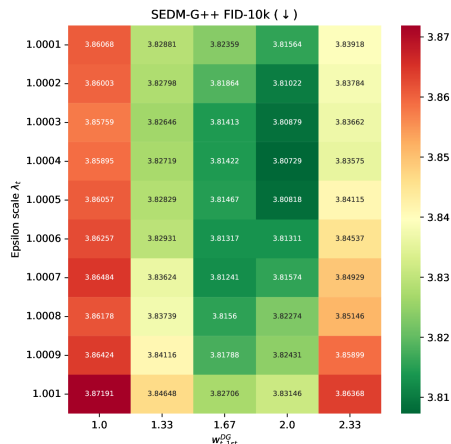


Figure 6. FID-10k ablation study on DG weight and scaling factor (Heun Solver).

prominent diffusion models is provided in Table 2. Given that our approach is based in the EDM model [18], it maintains a low Number of Function Evaluations (NFE) at 35 network calls per batch. This figure is significant as it directly relates to the computational cost associated with the sampling process.

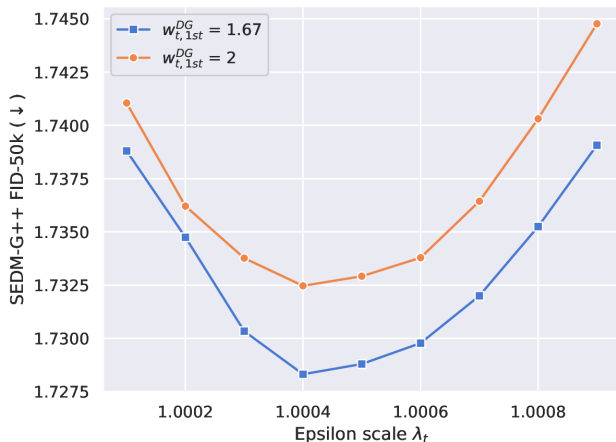


Figure 7. FID-50k ablation study on best performing DG weight values (Heun Solver).

An intriguing observation pertains to the fact that the FID gain achieved through Epsilon Scaling in the Euler sampler is more pronounced compared to the case of the Heun sampler. This is in line with the observations of Ning *et al.* [34], who attribute this phenomenon to two key factors. Firstly, higher-order ODE solvers, such as Heun solvers, entail a lower level of truncation error in contrast to Euler 1st order solvers. Secondly, the corrective steps integrated into the

Model	NFE(↓)	FID(↓)
VDM (Kingma <i>et al.</i> , 2021 [24])	1000	7.41
DDPM (Ho <i>et al.</i> , 2020 [15])	1000	3.17
iDDPM (Nichol & Dhariwal, 2021 [33])	1000	2.90
Soft Truncation (Kim <i>et al.</i> , 2022 [21])	2000	2.47
INDM (Kim <i>et al.</i> , 2022 [20])	2000	2.28
CLD-SGM (Dockhorn <i>et al.</i> , 2022 [12])	312	2.25
NCSN++ (Song <i>et al.</i> , 2020 [44])	2000	2.20
LSGM (Vahdat <i>et al.</i> , 2021 [45])	138	2.10
EDM (Karras <i>et al.</i> , 2022 [18])	35	1.97
EDM-G++ (Kim <i>et al.</i> , 2023 [22])	35	1.77
SEDM-G++ (ours)	35	1.73

Note: Following the work of Karras *et al.* [18], we calculate the FID for different seeds and report the minimum. Kim *et al.* [22] use random seeds for FID calculation. Manually calculating the FID of EDM-G++ results in an FID of 1.75.

Table 2. FID-50k performance comparison on unconditional CIFAR-10 image generation.

Heun solver serve to mitigate exposure bias by readjusting the drifted sampling trajectory back to the precise vector field. This is also evident in Fig. 2 and 3. In the case of the Heun solver, any prediction error (the root cause of exposure bias) incurred during each Euler step is rectified during the subsequent correction step (Fig. 3), leading to a reduction in exposure bias. This exposure bias perspective offers a comprehensive explanation for the superior performance of the Heun solver in diffusion models.

6. Conclusion

We explore the effectiveness of Discriminator Guidance in addressing exposure bias accumulation during the sampling process in diffusion models. Our findings reveal that, despite notable improvements in sample quality, Discriminator Guidance falls short in mitigating exposure bias. In response, we introduce SEDM-G++, a novel approach that integrates a modified sampling technique, incorporating both Discriminator Guidance and Epsilon Scaling. Applying this method to the pre-trained EDM model, we demonstrate its consistent ability to enhance sample quality while reducing exposure bias. This improvement is observed across various ODE solvers, a range of numbers of timesteps employed, and different hyperparameter settings. Our proposed approach outperforms the current state-of-the-art, achieving an FID score of 1.73 on the unconditional CIFAR-10 dataset.

Future Work In the ongoing expansion of this research, we intend to evaluate the applicability of this framework across a broader range of datasets, with past research suggesting a robust generalization to various domains [22, 34]. Exploring combinations of differ-

ent strategies to minimize exposure bias [26, 34, 35] has the potential to improve sample quality and also serves as a direction for future research. Furthermore, exploring the integration of a different state-of-the-art architecture for the discriminator part of the framework holds the potential for performance improvement.

References

- [1] Brian DO Anderson. Reverse-time diffusion equation models. *Stochastic Processes and their Applications*, 12(3):313–326, 1982. 3
- [2] Omri Avrahami, Dani Lischinski, and Ohad Fried. Blended diffusion for text-driven editing of natural images. In *Proceedings of the IEEE/CVF Conference on Computer Vision and Pattern Recognition*, pages 18208–18218, 2022. 2
- [3] Fan Bao, Chongxuan Li, Jun Zhu, and Bo Zhang. Analytic-dpm: an analytic estimate of the optimal reverse variance in diffusion probabilistic models. In *International Conference on Learning Representations*, 2021. 4
- [4] Fan Bao, Chongxuan Li, Jiacheng Sun, Jun Zhu, and Bo Zhang. Estimating the optimal covariance with imperfect mean in diffusion probabilistic models. In *International Conference on Machine Learning*, pages 1555–1584. PMLR, 2022. 4
- [5] Andreas Blattmann, Robin Rombach, Huan Ling, Tim Dockhorn, Seung Wook Kim, Sanja Fidler, and Karsten Kreis. Align your latents: High-resolution video synthesis with latent diffusion models. In *Proceedings of the IEEE/CVF Conference on Computer Vision and Pattern Recognition*, pages 22563–22575, 2023. 1, 2
- [6] Sam Bond-Taylor, Peter Hessey, Hiroshi Sasaki, Toby P Breckon, and Chris G Willcocks. Unleashing transformers: Parallel token prediction with discrete absorbing diffusion for fast high-resolution image generation from vector-quantized codes. In *European Conference on Computer Vision*, pages 170–188. Springer, 2022. 2
- [7] Nanxin Chen, Yu Zhang, Heiga Zen, Ron J Weiss, Mohammad Norouzi, and William Chan. Wavegrad: Estimating gradients for waveform generation. In *International Conference on Learning Representations*, 2020. 1, 2
- [8] Zijiao Chen, Jiaxin Qing, Tiange Xiang, Wan Lin Yue, and Juan Helen Zhou. Seeing beyond the brain: Conditional diffusion model with sparse masked modeling for vision decoding. In *Proceedings of the IEEE/CVF Conference on Computer Vision and Pattern Recognition*, pages 22710–22720, 2023. 2
- [9] Jooyoung Choi, Sungwon Kim, Yonghyun Jeong, Youngjune Gwon, and Sungroh Yoon. Ilvr: Conditioning method for denoising diffusion probabilistic models. In *Proceedings of the IEEE/CVF International Conference on Computer Vision*, pages 14367–14376, 2021. 2
- [10] Hyungjin Chung, Byeongsu Sim, and Jong Chul Ye. Come-closer-diffuse-faster: Accelerating conditional diffusion models for inverse problems through stochastic contraction. In *Proceedings of the IEEE/CVF Conference on Computer Vision and Pattern Recognition*, pages 12413–12422, 2022. 2
- [11] Prafulla Dhariwal and Alexander Nichol. Diffusion models beat gans on image synthesis. *Advances in neural information processing systems*, 34:8780–8794, 2021. 5
- [12] Tim Dockhorn, Arash Vahdat, and Karsten Kreis. Score-based generative modeling with critically-damped langevin diffusion. *arXiv preprint arXiv:2112.07068*, 2021. 7
- [13] Sicheng Gao, Xuhui Liu, Bohan Zeng, Sheng Xu, Yanjing Li, Xiaoyan Luo, Jianzhuang Liu, Xiantong Zhen, and Baochang Zhang. Implicit diffusion models for continuous super-resolution. In *Proceedings of the IEEE/CVF Conference on Computer Vision and Pattern Recognition*, pages 10021–10030, 2023. 2
- [14] Shuyang Gu, Dong Chen, Jianmin Bao, Fang Wen, Bo Zhang, Dongdong Chen, Lu Yuan, and Baining Guo. Vector quantized diffusion model for text-to-image synthesis. In *Proceedings of the IEEE/CVF Conference on Computer Vision and Pattern Recognition*, pages 10696–10706, 2022. 2
- [15] Jonathan Ho, Ajay Jain, and Pieter Abbeel. Denoising diffusion probabilistic models. In *Proceedings of the 34th International Conference on Neural Information Processing Systems*, pages 6840–6851, 2020. 1, 2, 3, 7
- [16] Jonathan Ho, Tim Salimans, Alexey Gritsenko, William Chan, Mohammad Norouzi, and David J Fleet. Video diffusion models. In *Advances in Neural Information Processing Systems*, pages 8633–8646, 2022. 1, 2
- [17] Bowen Jing, Gabriele Corso, Renato Berlinghieri, and Tommi Jaakkola. Subspace diffusion generative models. In *European Conference on Computer Vision*, pages 274–289. Springer, 2022. 2
- [18] Tero Karras, Miika Aittala, Timo Aila, and Samuli Laine. Elucidating the design space of diffusion-based generative models. *Advances in Neural Information Processing Systems*, 35:26565–26577, 2022. 1, 2, 5, 6, 7
- [19] Bahjat Kawar, Shiran Zada, Oran Lang, Omer Tov, Huiwen Chang, Tali Dekel, Inbar Mosseri, and Michal Irani. Imagic: Text-based real image editing with diffusion models. In *Proceedings of the IEEE/CVF Conference on Computer Vision and Pattern Recognition*, pages 6007–6017, 2023. 2
- [20] Dongjun Kim, Byeonghu Na, Se Jung Kwon, Dongsoo Lee, Wanmo Kang, and Il-chul Moon. Maximum likelihood training of implicit nonlinear diffusion model. *Advances in Neural Information Processing Systems*, 35:32270–32284, 2022. 7
- [21] Dongjun Kim, Seungjae Shin, Kyungwoo Song, Wanmo Kang, and Il-Chul Moon. Soft truncation: A universal training technique of score-based diffusion model for high precision score estimation. In *International Conference on Machine Learning*, pages 11201–11228. PMLR, 2022. 7
- [22] Dongjun Kim, Yeongmin Kim, Se Jung Kwon, Wanmo Kang, and Il-Chul Moon. Refining generative process with discriminator guidance in score-based diffusion models. In *Proceedings of the 40th International Conference on Machine Learning*, 2023. 1, 3, 5, 6, 7
- [23] Gwanghyun Kim, Taesung Kwon, and Jong Chul Ye. Diffusionclip: Text-guided diffusion models for robust image

- manipulation. In *Proceedings of the IEEE/CVF Conference on Computer Vision and Pattern Recognition*, pages 2426–2435, 2022. 2
- [24] Diederik Kingma, Tim Salimans, Ben Poole, and Jonathan Ho. Variational diffusion models. pages 21696–21707, 2021. 7
- [25] Zhifeng Kong, Wei Ping, Jiaji Huang, Kexin Zhao, and Bryan Catanzaro. Diffwave: A versatile diffusion model for audio synthesis. In *International Conference on Learning Representations*, 2020. 1, 2
- [26] Mingxiao Li, Tingyu Qu, Ruicong Yao, Wei Sun, and Marie-Francine Moens. Alleviating exposure bias in diffusion models through sampling with shifted time steps, 2023. 2, 3, 5, 8
- [27] Nan Liu, Shuang Li, Yilun Du, Antonio Torralba, and Joshua B Tenenbaum. Compositional visual generation with composable diffusion models. In *European Conference on Computer Vision*, pages 423–439. Springer, 2022. 2
- [28] Andreas Lugmayr, Martin Danelljan, Andres Romero, Fisher Yu, Radu Timofte, and Luc Van Gool. Repaint: Inpainting using denoising diffusion probabilistic models. In *Proceedings of the IEEE/CVF Conference on Computer Vision and Pattern Recognition*, pages 11461–11471, 2022. 2
- [29] Shitong Luo and Wei Hu. Diffusion probabilistic models for 3d point cloud generation. In *Proceedings of the IEEE/CVF Conference on Computer Vision and Pattern Recognition*, pages 2837–2845, 2021. 2
- [30] Chenlin Meng, Robin Rombach, Ruiqi Gao, Diederik Kingma, Stefano Ermon, Jonathan Ho, and Tim Salimans. On distillation of guided diffusion models. In *Proceedings of the IEEE/CVF Conference on Computer Vision and Pattern Recognition*, pages 14297–14306, 2023. 2
- [31] Ron Mokady, Amir Hertz, Kfir Aberman, Yael Pritch, and Daniel Cohen-Or. Null-text inversion for editing real images using guided diffusion models. In *Proceedings of the IEEE/CVF Conference on Computer Vision and Pattern Recognition*, pages 6038–6047, 2023. 2
- [32] Alexander Quinn Nichol and Prafulla Dhariwal. Improved denoising diffusion probabilistic models. In *Proceedings of the 38th International Conference on Machine Learning, ICML*, pages 8162–8171, 2021. 1, 2
- [33] Alexander Quinn Nichol and Prafulla Dhariwal. Improved denoising diffusion probabilistic models. In *International Conference on Machine Learning*, pages 8162–8171. PMLR, 2021. 7
- [34] Mang Ning, Mingxiao Li, Jianlin Su, Albert Ali Salah, and Itir Onal Ertugrul. Elucidating the exposure bias in diffusion models, 2023. 2, 3, 4, 5, 6, 7, 8
- [35] Mang Ning, Enver Sangineto, Angelo Porrello, Simone Calderara, and Rita Cucchiara. Input perturbation reduces exposure bias in diffusion models. In *International Conference on Machine Learning, ICML*, pages 26245–26265, 2023. 2, 3, 4, 5, 8
- [36] Konpat Preechakul, Nattanat Chatthee, Suttisak Wizadwongsa, and Supasorn Suwajanakorn. Diffusion autoencoders: Toward a meaningful and decodable representation. In *Proceedings of the IEEE/CVF Conference on Computer Vision and Pattern Recognition*, pages 10619–10629, 2022. 2
- [37] Marc’Aurelio Ranzato, Sumit Chopra, Michael Auli, and Wojciech Zaremba. Sequence level training with recurrent neural networks. In *4th International Conference on Learning Representations, ICLR 2016*, 2016. 2
- [38] Robin Rombach, Andreas Blattmann, Dominik Lorenz, Patrick Esser, and Björn Ommer. High-resolution image synthesis with latent diffusion models. In *2022 IEEE/CVF Conference on Computer Vision and Pattern Recognition (CVPR)*, pages 10674–10685. IEEE, 2022. 2, 5
- [39] Nataniel Ruiz, Yuanzhen Li, Varun Jampani, Yael Pritch, Michael Rubinstein, and Kfir Aberman. Dreambooth: Fine tuning text-to-image diffusion models for subject-driven generation. In *Proceedings of the IEEE/CVF Conference on Computer Vision and Pattern Recognition*, pages 22500–22510, 2023. 2
- [40] Florian Schmidt. Generalization in generation: A closer look at exposure bias. In *Proceedings of the 3rd Workshop on Neural Generation and Translation*, pages 157–167. Association for Computational Linguistics, 2019. 2
- [41] Jascha Sohl-Dickstein, Eric A Weiss, Niru Maheswaranathan, and Surya Ganguli. Deep unsupervised learning using nonequilibrium thermodynamics. In *Proceedings of the 32nd International Conference on International Conference on Machine Learning-Volume 37*, pages 2256–2265, 2015. 1, 2
- [42] Jiaming Song, Chenlin Meng, and Stefano Ermon. Denoising diffusion implicit models. In *International Conference on Learning Representations*, 2020. 2, 5
- [43] Yang Song and Stefano Ermon. Generative modeling by estimating gradients of the data distribution. *Advances in Neural Information Processing Systems*, 32, 2019. 1
- [44] Yang Song, Jascha Sohl-Dickstein, Diederik P. Kingma, Abhishek Kumar, Stefano Ermon, and Ben Poole. Score-based generative modeling through stochastic differential equations. In *9th International Conference on Learning Representations, ICLR 2021*, 2021. 1, 2, 3, 7
- [45] Arash Vahdat, Karsten Kreis, and Jan Kautz. Score-based generative modeling in latent space. *Advances in Neural Information Processing Systems*, 34:11287–11302, 2021. 7
- [46] Vikram Voleti, Alexia Jolicoeur-Martineau, and Chris Pal. Mcvd-masked conditional video diffusion for prediction, generation, and interpolation. *Advances in Neural Information Processing Systems*, 35:23371–23385, 2022. 1, 2
- [47] Su Wang, Chitwan Saharia, Ceslee Montgomery, Jordi Pont-Tuset, Shai Noy, Stefano Pellegrini, Yasumasa Onoe, Sarah Laszlo, David J Fleet, Radu Soricut, et al. Imagen editor and editbench: Advancing and evaluating text-guided image inpainting. In *Proceedings of the IEEE/CVF Conference on Computer Vision and Pattern Recognition*, pages 18359–18369, 2023. 2
- [48] Zhisheng Xiao, Karsten Kreis, and Arash Vahdat. Tackling the generative learning trilemma with denoising diffusion gans. In *International Conference on Learning Representations*, 2021. 4

- [49] Linqi Zhou, Yilun Du, and Jiajun Wu. 3d shape generation and completion through point-voxel diffusion. In *Proceedings of the IEEE/CVF International Conference on Computer Vision*, pages 5826–5835, 2021. [2](#)